

MODELING BURST TRAFFIC USING A *MAP* WITH A TREE STRUCTURE

Shoichi Nishimura
Tokyo University of Science

Miyuki Shinno
NTT Advanced Technology Corporation

(Received September 2, 2003; Revised March 9, 2004)

Abstract In this paper, a modeling approach for burst traffic using a *MAP* whose underlying process has a tree structure (*TSMAP*) is proposed. Characteristics of a *MAP/G/1* queue are analytically obtained. For large batch size, however, there are elaborate calculations. The spectral method is applied to overcome this problem. The rate matrix of a *TSMAP* is estimated by the EM algorithm. For a trace-driven simulation and our analytical model, probability density functions of the number of data units in the queueing system are quite similar. Using short-term dynamics of queueing system, the long-term dynamics is estimated.

Keywords: Queue, burst arrival, *MAP*, spectral method, EM algorithm, simulation

1. Introduction

In communication networks, both arrival rates and sizes of actual traffic data fluctuate widely. Recent studies have suggested that measured traffic exhibits a complex behavior like self-similarity or bursty, e.g. [13] and [26]. A Markovian arrival process (*MAP*) introduced by Neuts [19] is a versatile point process and its queueing model is highly tractable (see [19] and [14]). There are many literatures on network traffic modeling using a *MAP*, e.g. [1], [6], [12] and [27].

Let M be the number of phases of an underlying process for a *MAP*. For $k = 0, 1, 2, \dots$, let D_k and A_k be an $M \times M$ transition rate matrix with k batch arrivals and an $M \times M$ phase transition matrix with k arrivals during a service time, respectively. $A(z)$ and $D(z)$ are corresponding z -transforms. For a *MAP/G/1* queue, the calculation of a stationary probability distribution of a queue length needs two steps: The computation for a boundary vector of phase probabilities of the idle state at a service completion epoch and the computation for a stationary probability. For both steps, the Bini and Meini methods ([4], [5] and [15]) are effective among currently available methods applicable to a general *MAP*. However, the Bini and Meini methods or other analytical methods which need A_k are available only in limited batch size because large computation time is required. To overcome this difficulty, this paper proposes a spectral method based on eigenvalues and eigenvectors (see [8], [9], [10], [11], [16], [20], [21], [24], [22], [23], [25] and [28]). For the first step, a boundary vector is obtained by calculating M zeros of $\det(zI - A(z))$ in the unit disk (see [9], [10] and [11]). In order to find all zeros, high computational complexity is required, and there are few implementations for it using the spectral method. For the second step, the stationary probability is calculated using the fast Fourier inversion transform. In these two spectral methods, the stationary probability is calculated without A_k . For a birth-death modulated Markovian arrival process (*BDMAP*) introduced by Nishimura [23], it is demonstrated that eigenvalues of $D(z)$ are real and distinct. All M zeros in unit disk are precisely obtained

by the bisection method and the stationary probability is calculated precisely. As a natural extension of a *BDMMAP*, a tree structure *MAP* (*TSMAP*) is introduced in [22]. The effectiveness of the spectral methods for a *TSMAP* is also shown.

Bellcore Ethernet LAN trace (Available <http://ita.ee.lbl.gov/>) has bursty and shows a self-similar nature, e.g. [13]. For this trace, [27] discusses a fitting problem using their Markovian model that has an ON-OFF source whose sojourn time of OFF states are geometrically distributed. This model is also described as a *TSMAP*. And [1] proposes the fitting algorithm by considering the covariance structure of the input process and a superposition of heterogeneous two-state Markov modulated Poisson processes.

The main objective of this paper is to model Bellcore Ethernet trace by a *TSMAP*. From the frequency of the trace, data lengths are classified into four levels. Each level shows different characteristics. Using this classification, rate matrices D_k are estimated by the EM algorithm. For Markovian model, Asmussen et al. ([3] and [2]) proposed an estimation method for phase type distribution using the EM algorithm. Setting an assumption, we applied the EM algorithm to the estimation of D_k with a tree structure. For the estimated matrices, the stationary probability of the queue length of a *TSMAP/D/1* at an arbitrary time is calculated by the spectral methods. We focus on the probability density distribution of the queue length. For the trace-driven simulation and our analytical model, the probability density functions of the data units in the queueing system with a constant service time are derived. With this procedure, the short-term dynamics of queueing systems with different arrival rates are shown. From two discriminative short-term dynamics, the long-term dynamics is estimated using the concept of a “nearly completely decomposable” system. This system is originally introduced by Simon and Ando [29] for the area of economics and physics. And it is applied to queueing networks by Courtois [7]. Under this concept, systems of great size and complexity can be estimated using small subsystems. A nearly completely decomposable *TSMAP* over a long interval is constructed from two completely decomposable *TSMAPs* over the short-term intervals. From the second-order self-similarity, parameters for the long-term dynamics are determined.

In Section 2, our model is specified from data analysis. In Section 3, the rate matrix of a *TSMAP* is estimated by the EM algorithm. In Section 4, for a queueing analysis and a simulation, the distributions of the data units in the system are obtained. In Section 5, a nearly completely decomposable *TSMAP* is constructed by connecting two estimated *TSMAPs*. Numerical results are also given. The summary and concluding remarks are given in Section 6. In Appendix, the spectral methods for the computation of the queue length of a *TSMAP/G/1* and for the EM algorithm to estimate D_k are summarized. Note that terms “data length” and “packet” is used as “batch size” and “customer”, respectively throughout this paper.

2. The Model Specification

In this section, our model is specified from the data analysis of Bellcore Ethernet LAN trace. The trace consists of the arrival time in seconds and the data length in bytes. Note that one byte (not one packet) is regarded as one arrival of the input process and consider various data length. The total number of packet arrivals is one million. The first 7 data are in Table 1: the length of first arrival packet is 87.

The whole one million packets is divided into ten parts, and the arrival rate of data units per second for each 100,000 packets is calculated as shown in Table 2. In later discussions, we call the arrival rate of data units as the arrival rate λ simply.

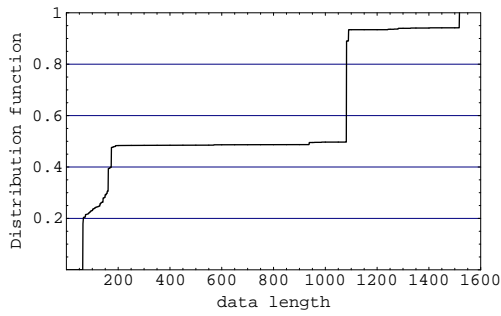


Figure 1: Distribution of data length

Table 3: Number of transitions between levels

| $i \backslash j$ | 2 | 3 | 4 | 5 |
|------------------|--------|-------|--------|-------|
| 2 | 145103 | 52921 | 96328 | 11366 |
| 3 | 60561 | 68355 | 42833 | 9017 |
| 4 | 91493 | 53929 | 297550 | 10113 |
| 5 | 8560 | 5561 | 16374 | 29935 |

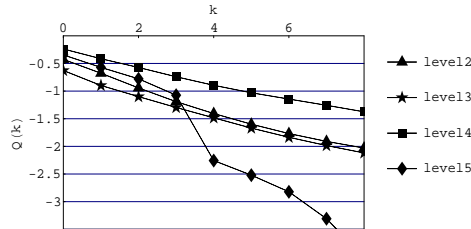


Figure 2: Number of successive visits to the same level

It is found that the arrival rate is unsteady, and traffic seems to be a non-stationary process. The lowest arrival rate 254919.0 is about half of the highest one 543780.4. Denote these time subintervals $(0, 210.761734)$ and $(1222.526978, 1354.025757)$ as Interval I and II, respectively. Next, the distribution of the Ethernet data length is illustrated in Figure 1 whose horizontal and vertical axes are the data length and the cumulative distribution function, respectively. The Ethernet LAN trace includes some large data lengths, e.g. lengths of 1518, 1330, and the arrival rate varies widely from high to low. The frequency of particular data lengths is high: the frequency of 1082 is about 40 % for this trace. From this result, the data length is classified into 4 levels as

- level 2 $0 < x \leq 160$
- level 3 $160 < x \leq 600$
- level 4 $600 < x \leq 1300$
- level 5 $1300 < x$.

Table 2 shows the number of arriving packets among 1,000,000 whose starting and terminating levels are i and j ($i, j = 2, \dots, 5$), respectively. For example, the first transition is from level 2 ($x = 87$) to level 2 ($x = 142$), and the two successive visits to level 4 accounts for about 30 % of whole 999,999 transitions.

Let $q_i(n)$ be the probability of the n times of successive visits to level i without visiting other levels. The distribution is illustrated in Figure 2 where horizontal and vertical axes are the number of successive times k and $Q(k) = \log_{10}(1 - \sum_{n=0}^k q_i(n))$, respectively. Approximately, $(1 - \sum_{n=0}^k q_i(n))$ are decreasing geometrically because $Q(k)$ is almost linearly decreasing except for level 5.

Let $F_{i,j}(t)$ be the probability that the inter-arrival time is less than or equal to t , given that the starting and the terminating levels are i and j , respectively. When $F_{i,j}(t)$ is ex-

Table 1: The first 7 data

| | | | | | | | |
|------------|----------|----------|----------|----------|----------|----------|----------|
| A.T.(sec.) | 0.017716 | 0.036760 | 0.036844 | 0.047196 | 0.051132 | 0.051292 | 0.052872 |
| D.L.(byte) | 87 | 142 | 64 | 1518 | 1518 | 162 | 1330 |

ponential with the parameter λ , $\log(1 - F_{i,j}(t))$ is a straight line which goes through the origin with the slope $-\lambda$. Similarly, when $F_{i,j}(t)$ is a mixture of two exponential distributions, the curve $\log(1 - F_{i,j}(t))$ is piecewise linear approximately. In Figure 3, we illustrate $\log(1 - F_{i,i}(t))$ with the horizontal axis t where the starting and the terminating levels are same. From shapes of these curves, $F_{2,2}(t)$ seems to be the mixture of exponential distributions with positive weights and $F_{3,3}(t)$, $F_{4,4}(t)$ and $F_{5,5}(t)$ with negative weights.

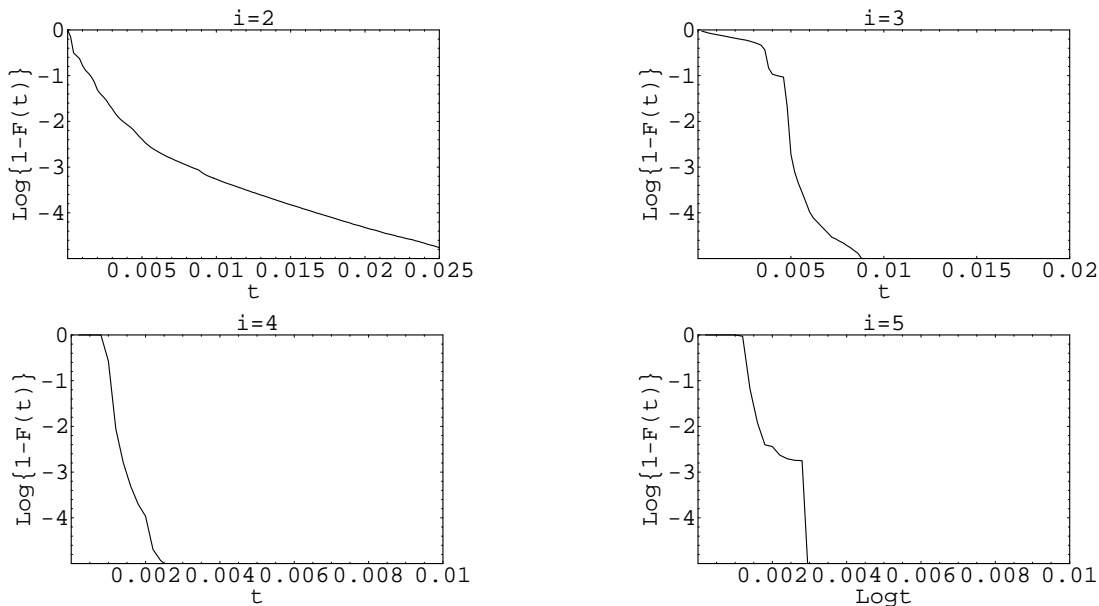


Figure 3: $\log(1 - F_{i,i}(t))$ for $i = 2, \dots, 5$

Define a terminating phase of the inter-arrival time as the phase of the underlying process just after an arrival occurs. For the construction of the EM algorithm, the following assumption is set.

Assumption 1

For each data length k , there exists the unique terminating phase $i = i(k)$.

The intermediate phase of the underlying process is unobservable. However, setting the above assumption may enable us to observe starting and terminating phases of each inter-

Table 2: Data partitioning

| Packets | Observed time(sec.) | Arrival rate(byte/sec.) | |
|---------------------|---------------------------|-------------------------|----|
| 1 ~ 100,000 | 0 ~ 210.761734 | 254919.0 | I |
| 100,001 ~ 200,000 | 210.761734 ~ 397.429688 | 302264.0 | |
| 200,001 ~ 300,000 | 397.429688 ~ 586.055186 | 301981.8 | |
| 300,001 ~ 400,000 | 586.055186 ~ 801.676697 | 299403.5 | |
| 400,001 ~ 500,000 | 801.676697 ~ 1025.821045 | 267992.3 | |
| 500,001 ~ 600,000 | 1025.821045 ~ 1222.526978 | 338251.3 | II |
| 600,001 ~ 700,000 | 1222.526978 ~ 1354.025757 | 543780.4 | |
| 700,001 ~ 800,000 | 1354.025757 ~ 1485.907593 | 533277.2 | |
| 800,001 ~ 900,000 | 1485.907593 ~ 1623.599487 | 501980.2 | |
| 900,001 ~ 1,000,000 | 1623.599487 ~ 1759.620972 | 507785.7 | |
| 1 ~ 1,000,000 | 0 ~ 1759.620972 | 362742.8 | |

arrival time from the data length. As discussed in Appendix C, the EM algorithm for a *MAP* can be constructed and by using the spectral method the infinitesimal generator of a *TSMAP* can be estimated effectively.

For specifying a *TSMAP*, three points are considered as follows:

- (a) Assumption 1 is satisfied.
- (b) $q_i(l)$ is approximated as a geometrical distribution.
- (c) $F_{i,i}(t)$ $i = 2, \dots, 5$ are approximated as a generalized hyper-exponential distribution. That is, the coefficients for mixing weight are allowed to be negative. In case $i = 2$ and in case $i = 3, 4, 5$, $F_{i,i}(t)$ have positive and negative mixing weights, respectively.

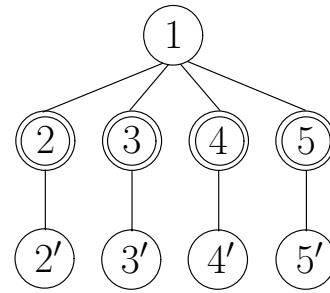


Figure 4: Tree structure of the underlying process

From (a), the terminating phase of arrivals in level i is phase i . From (b), we assume that all terminating phases ($i = 2, \dots, 5$) are connected with the phase 1 which is the root node of the graph with a tree structure. From (c), for each terminating phase i , the phase i' is added in order to represent a hyper-exponential distribution. Assume that $1, 2, 2', \dots, 5, 5'$ are arranged as a tree graph illustrated in Figure 4, where a double circle with phase i represents a terminating phase i . For $i = 2, \dots, 5$, let $f_i(z)$ be the generating function of the data length when an arrival occurs at $(1, i)$, (i, i) , (i', i) -transitions. From the distribution of the data length in Figure 1, we set

$$\begin{aligned} f_2(z) &= 0.5z^{64} + 0.17z^{80} + 0.08z^{110} + 0.25z^{140} \\ f_3(z) &= z^{173}, f_4(z) = z^{1082}, f_5(z) = z^{1518}. \end{aligned} \quad (1)$$

3. The EM Algorithm

In statistics, the EM algorithm has been widely used as parameter estimation from incomplete data. This algorithm consists of two steps: Expectation Step (E-Step) and Maximization Step (M-Step). In the E-step, given the observed data and the previously estimated parameters, the conditional expectations of the sufficient statistics are computed. And in the M-step, using the conditional expectations calculated in the E-step, the likelihood is maximized. These two steps are repeated alternately.

For Markovian models, Asmussen et al.([3] and [2]) apply the EM algorithm to the estimation of an initial vector and a rate matrix for a phase-type distribution from the sequence of the inter-arrival time. From the trace, we can not observe intermediate phase transition epochs, so the initial vector and the infinitesimal generator are estimated from incomplete data.

Now, return to our model. The term “level” in the previous section is regarded as “phase” of a *MAP*. For the first 7 packets of 1,000,000, the starting phase (S.P.) i , the terminating phase (T.P.) j and the inter-arrival time (I-A.T.) y of the underlying process are given in Table 4.

From the data set (i^ν, j^ν, y^ν) ($\nu = 1, \dots, N$), the infinitesimal generator of the underlying process with the specified structure is estimated by the EM algorithm. For details, see Appendix C.

Table 4: S.P., T.P. and I-A.T.

| | | | | | | | |
|--------|---------|---------|---------|---------|---------|--------|--------|
| S.P. | – | 2 | 2 | 2 | 5 | 5 | 3 |
| T.P. | 2 | 2 | 2 | 5 | 5 | 3 | 5 |
| I-A.T. | .017716 | .019044 | .000084 | .010352 | .003936 | .00016 | .00158 |

4. Numerical Results of 100,000 Packets

In this section, we analyze the data over the intervals with the lowest and the highest arrival rates in Table 2, i.e. Interval I and II.

4.1. Interval I

For Interval I, let $S^{(1)} = \{s_{i,j}^{(1)}\}$ and $T^{(1)} = \{t_{i,j}^{(1)}\}$ be transition rate matrices with and without arrival, respectively. From data set (i^ν, j^ν, y^ν) , $\nu = 1, \dots, 100,000$, using the EM algorithm in Appendix C, $S^{(1)}$ and $T^{(1)}$ are estimated as

$$S^{(1)} = \begin{matrix} i \backslash j & 1 & 2 & 2' & 3 & 3' & 4 & 4' & 5 & 5' \\ \begin{matrix} 1 \\ 2 \\ 2' \\ 3 \\ 3' \\ 4 \\ 4' \\ 5 \\ 5' \end{matrix} & \begin{pmatrix} 0 & 2.80E3 & 0 & 1.38E3 & 0 & 9.59E-9 & 0 & 2.936E-14 & 0 \\ 0 & 4.02E1 & & & & & & & \\ 0 & 2.26E2 & & & & & & & \\ & & 0 & 7.86E-2 & & & & & \\ & & 0 & 2.56E2 & & & & & \\ & & & & 0 & 4.596E-12 & & & \\ & & & & 0 & 1.47E3 & & & \\ & & & & & & 0 & 3.856E-20 & 0 \\ & & & & & & 0 & 6.66E2 & 0 \end{pmatrix} \end{matrix},$$

$$T^{(1)} = \begin{matrix} i \backslash j & 1 & 2 & 2' & 3 & 3' & 4 & 4' & 5 & 5' \\ \begin{matrix} 1 \\ 2 \\ 2' \\ 3 \\ 3' \\ 4 \\ 4' \\ 5 \\ 5' \end{matrix} & \begin{pmatrix} -2.41E4 & 4.29E3 & & 3.28E3 & & 1.12E4 & & 1.16E3 & \\ 2.48E3 & -3.32E3 & 7.97E2 & & & & & & \\ & 1.67E1 & -2.43E2 & & & & & & \\ 4.39E3 & & & -7.24E3 & 2.85E3 & & & & \\ & & & 9.76E1 & -3.54E2 & & & & \\ 4.88E3 & & & & & -6.88E3 & 2.00E3 & & \\ & & & & & 1.21E-3 & -1.47E3 & & \\ 5.50E3 & & & & & & & -1.06E4 & 5.09E3 \\ & & & & & & & 7.45E-6 & -6.66E2 \end{pmatrix} \end{matrix}.$$

For $i = 2, 3$ $s_{1,i}^{(1)} > \max(s_{i,i}^{(1)}, s_{i',i}^{(1)})$ and for $i = 4, 5$ $s_{i',i}^{(1)} \gg \max(s_{1,i}^{(1)}, s_{i,i}^{(1)})$. For $i = 4, 5$, $t_{i,i}^{(1)}$ are large, whereas $t_{i',i}^{(1)}$ is almost zero. This shows that additional phases 4' and 5' play an important role and the path of phase transition

$$i \rightarrow i' \rightarrow i \quad (*)$$

occurs when large data length ($i = 4, 5$) appears within a short time. From Assumption 1 and equation (1), $D^{(1)}(z) = \{d_{i,j}^{(1)}(z)\}$ is given as

$$d_{i,j}^{(1)}(z) = t_{i,j}^{(1)} + s_{i,j}^{(1)} f_j(z).$$

Next, the fitting of z -transform $D^{(1)}(z)$ is evaluated. Real packet stream is transmitted through a queueing system. As a criterion of fitting evaluation, we consider the probability density function of the number of data units waiting in the system. Note that for an ordinal analysis of the queue length of a $MAP/G/1$, a service completion epoch is treated as an observing point, while an arbitrary time is considered here. For Bellcore LAN trace, we run a simulation for the single server queue with a constant service rate. And an analytical result for a $TSMAP/D/1$ queue is derived by spectral methods in Appendix B.

For $\lambda = 254919.0$ and $\rho = 0.254919$, the probability density functions p_n ($n = 0, 1, 2, \dots$) for both the simulation and the analytical model are calculated. From Little's formula, idle probabilities at an arbitrary time for them are same $p_0 = 0.7451$ in our numerical results. Compared with this value, p_n ($n = 1, 2, \dots$) is relatively small. So the probability density functions without the idle probability are illustrated in Figures 5 and 6. From the same reason, the idle probability is omitted from the figures of this type in the following section. The mean, the standard deviation, the coefficient of variation, and the idle probability are given in Table 4.1.

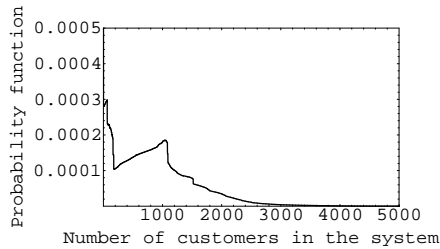


Figure 5: Bellcore trace for Interval I

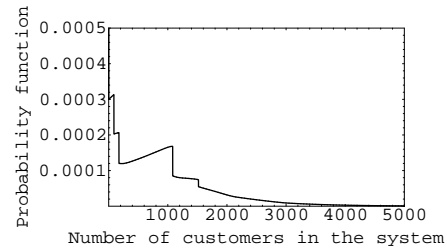


Figure 6: TSMAP for Interval I

Table 5: Characteristics for Interval I ($\rho = 0.25$)

| | Bellcore | TSMAP |
|----------|----------|--------|
| mean | 226.5 | 244.3 |
| s.d. | 515.7 | 600.1 |
| c.v. | 2.277 | 2.456 |
| Pr(idle) | 0.7451 | 0.7451 |

Table 6: Characteristics for Interval II ($\rho = 0.54$)

| | Bellcore | TSMAP |
|----------|----------|--------|
| mean | 733.0 | 821.1 |
| s.d. | 1143 | 1225 |
| c.v. | 1.560 | 1.492 |
| Pr(idle) | 0.4562 | 0.4562 |

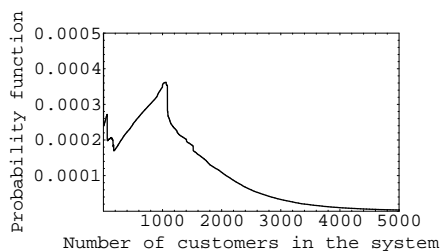


Figure 7: Bellcore trace for Interval II ($\rho = 0.54$)

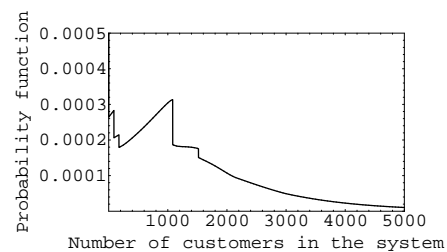


Figure 8: TSMAP for Interval II ($\rho = 0.54$)

4.2. Interval II

For Interval II, the same tree structure previously specified is used and the infinitesimal generator is estimated by the same procedure for Interval I.

Let $S^{(2)} = \{s_{i,j}^{(2)}\}$ and $T^{(2)} = \{t_{i,j}^{(2)}\}$ be rate matrices with arrival and without arrival, respectively. Using the EM algorithm, from the data set $(i^\nu, j^\nu, y^\nu), \nu = 600, 001, \dots, 700, 000$,

$S^{(2)}$ and $T^{(2)}$ are estimated as

$$S^{(2)} = \begin{pmatrix} 0 & 3.20E3 & 0 & 1.13E3 & 0 & 3.44E-5 & 0 & 2.83E-9 & 0 \\ 0 & 1.99E2 & & & & & & & \\ 0 & 2.16E2 & & & & & & & \\ & & 0 & 1.17E1 & & & & & \\ & & 0 & 2.63E2 & & & & & \\ & & & & 0 & 1.63E-8 & & & \\ & & & & 0 & 1.47E3 & & & \\ & & & & & & 0 & 1.13E-13 & 0 \\ & & & & & & 0 & 7.82E2 & 0 \end{pmatrix},$$

$$T^{(2)} = \begin{pmatrix} -2.57E4 & 3.49E3 & & 2.75E3 & & 1.33E4 & & 1.86E3 & & \\ 3.62E3 & -4.37E3 & 5.50E2 & & & & & & & \\ & 1.32E1 & -2.30E2 & & & & & & & \\ 7.27E3 & & & -8.82E3 & 1.54E3 & & & & & \\ 4.74E3 & & & 7.36E1 & -3.36E2 & & & & & \\ 7.04E3 & & & & & -7.56E3 & 2.82E3 & & & \\ & & & & & 1.71E-3 & -1.47E3 & & & \\ & & & & & & & -1.16E4 & 4.56E3 & \\ & & & & & & & 4.47E-5 & -7.82E2 & \end{pmatrix}.$$

As defined before,

$$d_{i,j}^{(2)}(z) = t_{i,j}^{(2)} + s_{i,j}^{(2)} f_j(z).$$

Similar to Interval I, for Interval II, the large data length ($i = 4, 5$) appears within a short time through the path (*). On the other hand, the arrival rate of 100,000 packets for Interval II is almost twice as high as that of the first one. For $\lambda = 543780.4$ and $\rho = 0.5437804$, the probability density functions are shown in Figures 7 and 8. Those characteristics are shown in Table 4.1 which differs from that of Interval I. For example, see $t_{1,i}^{(1)}$ and $t_{1,i}^{(2)}$, $i = 2, 3, 4, 5$: $t_{1,2}^{(1)} > t_{1,2}^{(2)}$, $t_{1,3}^{(1)} > t_{1,3}^{(2)}$, $t_{1,4}^{(1)} < t_{1,4}^{(2)}$ and $t_{1,5}^{(1)} < t_{1,5}^{(2)}$. This means that Interval I intends to visit phase 2 or 3 frequently, whereas Interval II intends to visit phase 4 or 5. These results are also predicted from Table 1.

5. A Nearly Completely Decomposable *TSMAP*

In the previous section, we estimate two *TSMAPs* from the short-term data: 100,000 packets. There are several differences between components of $D^{(1)}(z)$ and $D^{(2)}(z)$. In this section, we attempt at estimating whole data from the results of two discriminative intervals, i.e. intervals with the lowest and the highest arrival rates.

Simon and Ando [29] introduce the concept of a “nearly completely decomposable” system and apply it to economics, physics etc. The principal idea of this system is as follows: for each subsystem, the intragroup interaction may be defined as if the intergroup interaction did not exist, and the intergroup interaction may be defined independently of the intragroup interaction. This concept is used as a technique in order to evaluate the dynamics of systems of great size and complexity. And it is applied to queueing networks and computer systems by Courtois [7].

Using the concept of a nearly completely decomposable system, a nearly completely decomposable *TSMAP* is constructed from the two heterogeneous *TSMAPs* in this section. As illustrated in Figure 9, the phase 0 connects two *TSMAPs* and is the root node of the graph with new tree structure. Note that a tree structure is preserved under this construction.

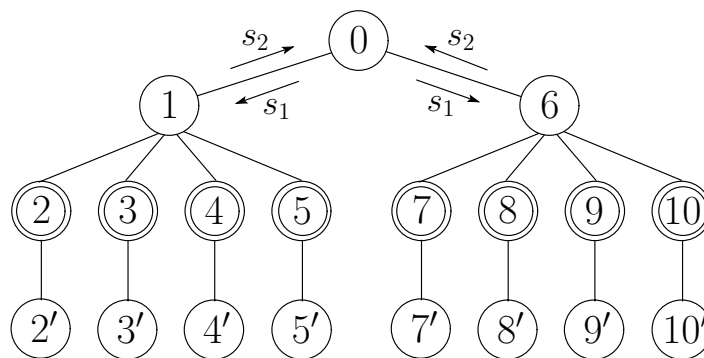


Figure 9: A nearly completely decomposable system with tree structure

The rate matrix $D(z)$ corresponding to this new *TSMAP* is composed of two matrices $D^{(1)}(z)$ and $D^{(2)}(z)$ on the diagonal. The explicit representation is

$$D(z) = \begin{bmatrix} 0 & \mathbf{0} & \mathbf{0} \\ \mathbf{0}^T & D^{(1)}(z) & \mathbf{0} \\ \mathbf{0}^T & \mathbf{0} & D^{(2)}(z) \end{bmatrix} + \begin{bmatrix} -2s_1 & s_1 & \mathbf{0} & s_1 & \mathbf{0} \\ s_2 & -s_2 & & & \\ \mathbf{0}^T & \mathbf{0} & & \mathbf{0} & \\ s_2 & & & -s_2 & \\ \mathbf{0}^T & \mathbf{0} & & \mathbf{0} & \end{bmatrix},$$

where s_1 and s_2 connecting two short-time *TSMAPs* have an influence on long-term dynamics.

The second-order self-similarity

It is recognized that the measured network traffic shows the self-similar nature. In particular, the second-order self-similarity is widely studied, e.g. [13]. This property is shown by considering the aggregated processes of LAN trace. Here we use following expressions. Let $X(0, T)$ and $\text{Var}[X(0, T)]$ be the number of arrivals during $(0, T)$ and its variance in the stationary version, respectively. If arrivals are formulated as an asymptotically second-order self-similar process with the Hurst parameter $H = 1 - \beta/2$ ($1 > \beta > 0$), then

$$\log_{10}(\text{Var}[X(0, T)]/T) \approx (1 - \beta) \times \log_{10} T + \log_{10} \sigma^2. \tag{2}$$

So, $\log_{10}(\text{Var}[X(0, T)]/T)$ is approximated by a linear function of $\log_{10} T$ with slope $(1 - \beta)$.

To observe the second-order self-similarity of LAN trace, we consider an aggregated process $X_i(T)$ of the number of data units during $((i - 1)T, iT]$. Define the variance of $\{X_i(T); i = 1, \dots, n\}$ as $\text{Var}[X(0, T)]$. For $T = 10^{-n}$ ($n = -2, \dots, 2$), $\log_{10}(\text{Var}[X(0, T)])$ is illustrated in Figure 10, whose horizontal axis is $\log_{10} T$. The length of the linear segment with a positive slope is considered as the time scale of the second-order self-similarity. The time scale of LAN trace seems to be greater than 4.

For a MAP, the variance $\text{Var}[X(0, T)]$ of the aggregated process is analytically derived in [17] and [28]. Here we consider the second-order self-similarity as the criterion for determining s_1 and s_2 . When $s_1 = 100$ and $s_2 = 0.1$, the solid line fits well with the dotted line in Figure 10. In this case, the arrival rate of the nearly completely decomposable *TSMAP* is 384477.4. It also fits with that of all the 1,000,000 packets (362742.8 in Table 2).

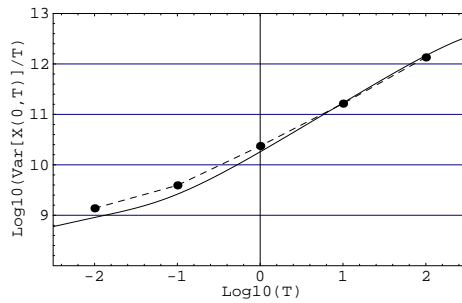


Figure 10: Second-order self-similarity
 - - - Bellcore, — TSMAP

Numerical results of 1,000,000 packets

Finally, we make an analysis of long-term dynamics for 1,000,000 packets for $\rho = 0.36$ and 0.5, i.e. same traffic intensity and higher one. For each distribution, the mean, the standard deviation, the coefficient of variation, and the idle probability at an arbitrary time are given in Table 8. For $\rho = 0.36$, the probability density functions are illustrated in Figures 11,12 and the value of the density p_n and the cumulative distribution function $F(n)$ are given in Table 7. Each value of analytical model fit well to that of simulation results. For $\rho = 0.5$, the probability density functions are illustrated in Figures 13,14. This case may needs a modification of the model.

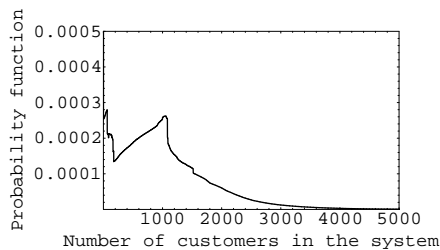


Figure 11: Bellcore trace for whole interval
 ($\rho = 0.36$)

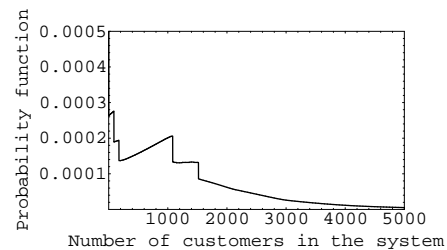


Figure 12: TSMAP for whole interval
 ($\rho = 0.36$)

Table 7: Probability and distribution function for $\rho = 0.36$

| n | p_n | | $F(n)$ | |
|-------|----------|----------|----------|--------|
| | Bellcore | TSMAP | Bellcore | TSMAP |
| 1 | 2.533E-4 | 2.632E-4 | 0.6375 | 0.6375 |
| 10 | 2.559E-4 | 2.645E-4 | 0.6398 | 0.6399 |
| 100 | 2.117E-4 | 1.901E-4 | 0.6619 | 0.6633 |
| 1000 | 2.569E-4 | 2.012E-4 | 0.8387 | 0.8144 |
| 10000 | 6.649E-8 | 1.093E-7 | 0.9999 | 0.9999 |

6. Concluding Remarks

In this study, a modeling procedure of burst traffic using a *MAP* is proposed. Our model allows for relatively large batch arrivals. Bellcore Ethernet LAN trace is used as raw data. The

| ρ | 0.36 | | 0.5 | |
|----------|----------|--------|----------|--------|
| input | Bellcore | TSMAP | Bellcore | TSMAP |
| mean | 382.7 | 485.5 | 2360 | 1229 |
| s.d. | 714.6 | 975.6 | 4092 | 2099 |
| c.v. | 1.867 | 2.010 | 1.734 | 1.708 |
| Pr(idle) | 0.6372 | 0.6372 | 0.5009 | 0.5000 |

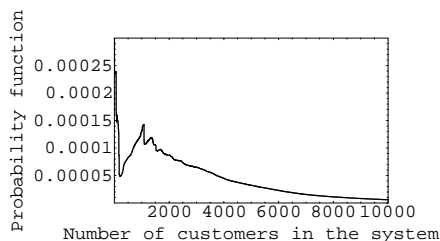


Figure 13: Bellcore trace for whole interval
($\rho = 0.5$)

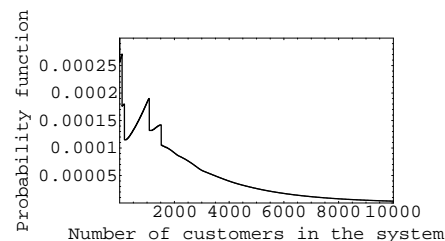


Figure 14: TSMAP for whole interval
($\rho = 0.5$)

maximum Ethernet data length is 1518. In order to deal with such large data length, enormous calculations are required, particularly the calculation of A_k . Considering a *TSMAP* and using three spectral methods in Appendix B, this difficulty is overcome.

First, by classifying the data length into levels and setting Assumption 1, the detailed structure of a *TSMAP* in Figure 4 is specified. Next, the infinitesimal generator of the underlying process is estimated by the EM algorithm. It should be noted that the tree structure is preserved through iterations. By applying the spectral method for the EM algorithm, the result is obtained after 26 iterations for 100,000 packet arrivals. The computing time required for each iteration is about 20 minutes on a 1.5GHz Pentium processor with 512 MB RAM, which is shorter than that of the Runge-Kutta method in [3].

The spectral method is very useful although it needs the assumption of distinct eigenvalues. In our model, as a numerical results, the following three types of eigenvalues are distinct; eigenvalues of T , all zeros $zI - A(z)$ on the unit disk and for each z on the unit circle and all eigenvalues $D(z)$. That is to say, Assumption 2 is satisfied numerically. In our experiments, we have never encountered the multiple eigenvalues for the other *TSMAP* models, so the Assumption 2 seems not so strong in applications.

We focus on the density function of the queue length, not the cumulative distribution. For the trace-driven simulation and our analytical model, the probability density functions are quite similar. It is notable that our newly method can calculate the probability density function of the queue length precisely even though there are large batch arrivals which other methods can not deal with. However, the long-term dynamics of a queueing system is not predicted well in Section 5. That is, the influence of parameters s_1 and s_2 on the distribution remains unclear. With regard to this attempt, these points should be refined.

Appendix

A. A Markovian Arrival Process

Consider a Markovian arrival process (*MAP*) introduced by Neuts [19] on a state space $\{i : i = 1, \dots, M\}$ whose underlying process has an infinitesimal generator $D = D(1)(D(z)$ is defined below). Assume that for $|z| \leq 1$, the z -transform of rate matrices $D(z) = \sum_{k=0}^{\infty} D_k z^k$ is analytic. Let $\boldsymbol{\pi} = (\pi_1, \pi_2, \dots, \pi_M)$ be the stationary probability vector of D ($\boldsymbol{\pi}D = \mathbf{0}$ and $\boldsymbol{\pi}\mathbf{e} = 1$). The mean arrival rate is $\lambda = \boldsymbol{\pi}D(1)\mathbf{e} = \boldsymbol{\pi} \sum_{k=1}^{\infty} kD_k\mathbf{e}$, where \mathbf{e} is the 1s column vector. Let $H(t)$ be the distribution function of a service time with a mean μ^{-1} . Let $h(\alpha) = \int_0^{\infty} e^{\alpha t} dH(t)$ and $h^{-1}(z)$ be the moment generating function of a service time and its inverse function, respectively. Then $A(z) \triangleq \sum_{k=0}^{\infty} A_k z^k = \int_0^{\infty} e^{D(z)t} dH(t)$ is the probability generating matrix function of the number of arrivals during a service time. Assume that the traffic intensity $\rho = \frac{\lambda}{\mu} < 1$.

Let $\mathbf{p}_n = (p_{n,1}, \dots, p_{n,M})$ ($n \geq 0$) be the M -dimensional row vector whose i th entry is the stationary joint probability that an arrival phase is i and the number of customers in the system is n at an arbitrary time. Let G and \mathbf{g} be the phase transition stochastic matrix of the first passage time from the level $n+1$ to the level n and its invariant probability vector ($\mathbf{g}G = \mathbf{g}$, $\mathbf{g}\mathbf{e} = 1$), respectively. The probability generating function $\mathbf{p}(z)$ is given by

$$\mathbf{p}(z) = \lambda^{-1}(1 - \rho)\mathbf{g}(z - 1)A(z)(zI - A(z))^{-1},$$

see [14]. Let $\alpha_i(z)$ ($i = 1, \dots, M$) be the eigenvalues of $D(z)$ and $\mathbf{u}_i(z)$ and $\mathbf{v}_i(z)$ be corresponding normalized left and right eigenvectors: $\mathbf{u}_i(z)D(z) = \alpha_i(z)\mathbf{u}_i(z)$ and $D(z)\mathbf{v}_i(z) = \alpha_i(z)\mathbf{v}_i(z)$. Particularly, $\alpha_1(1) = 0$, $\mathbf{u}_1(1) = \boldsymbol{\pi}$ and $\mathbf{v}_1(1) = \mathbf{e}$. To simplify our discussion, the following regularity condition is set.

Assumption 2

All eigenvalues $\alpha_i(z)$ ($i = 1, \dots, M$) discussed in this paper are simple.

B. The Spectral Methods for the Stationary Probability

For a *BDMMAP* and a *TSMAP*, spectral methods for the calculation of the probability of the queue length at a service completion epoch are in [22] and [23]. The probability of the queue length at an arbitrary time is derived by its easy modification.

Calculation of the matrix G

For the calculation of a stationary probability \mathbf{p}_n , numerically precise values of the vector \mathbf{g} is necessary. Let z_i ($i = 1, \dots, M$) and $\boldsymbol{\eta}_i$ be zeros of $\det(zI - A(z))$ on the unit disk and a corresponding right null vector of $zI - A(z)$, respectively. It is proved there exist M zeros of $\det(zI - A(z))$ in the unit disk ([9], [10], [11]). For $z_1 = 1$, we put $\boldsymbol{\eta}_1 = \mathbf{e}$. Define the matrix Y as $Y = [\boldsymbol{\eta}_1, \dots, \boldsymbol{\eta}_M]$.

Proposition 1 *The matrix Y is nonsingular and*

$$G = Y \begin{bmatrix} z_1 & & \\ & \ddots & \\ & & z_M \end{bmatrix} Y^{-1}.$$

Calculation of the stationary probability

Using the fast Fourier inversion transform of the probability generating function $\mathbf{p}(z)$, the spectral method for the calculation of a stationary vector \mathbf{p}_n is given.

Proposition 2 For a sufficiently large N_1 , let $\omega = e^{i2\pi/N_1}$. Then

$$\mathbf{p}_n \approx \frac{\lambda^{-1}(1-\rho)\mathbf{g}}{N_1} \sum_{k=0}^{N_1-1} V(\omega^k) \begin{bmatrix} \frac{(\omega^k-1)h(\alpha_1(\omega^k))}{\omega^k-h(\alpha_1(\omega^k))} & & \\ & \dots & \\ & & \frac{(\omega^k-1)h(\alpha_M(\omega^k))}{\omega^k-h(\alpha_M(\omega^k))} \end{bmatrix} U(\omega^k)\omega^{-kn}$$

In this equation, for $k=0$ and $i=1$, we define as $\frac{(\omega^k-1)h(\alpha_i(\omega^k))}{\omega^k-h(\alpha_i(\omega^k))} = \frac{1}{1-\rho}$. The probability of the queue length n at an arbitrary time is given by $p_n = \mathbf{p}_n \mathbf{e}$.

C. The Spectral Method for the EM Algorithm

In [3] and [2], Asmussen introduced the EM algorithm for the phase type distribution. The components of an initial vector and a phase transition matrix are estimated using an inter-arrival time as observed incomplete data. Based on this idea, the transition rate matrix of a MAP are estimated under Assumption 1. Denote $S = (s_{k,l}) \equiv \sum_{n=1}^{\infty} D_n$ and $T = (t_{k,l}) \equiv D - S$ as the transition rate matrices with and without arrival, respectively. From observed incomplete data $\{(i^\nu, j^\nu, y^\nu) \mid \nu = 1, \dots, N\}$, where i^ν and j^ν are the starting and the terminating phase during the ν th inter-arrival time y^ν . That is, an intermediate phase transition is estimated from an inter-arrival time. In equations below, the superscript t represents the eigenvalue and the eigenvector of T , i.e. α_i^t , \mathbf{u}_i^t , and \mathbf{v}_i^t . Let Z_k be the total time spent in phase k . Let $M_{k,l}$ and $N_{k,l}$ be the number of transitions from k to l without and with arrival, respectively. Spectral representations are derived as follows:

$$\begin{aligned} a_j(i, y; S, T) &\triangleq \mathbf{e}_i^T \exp(Ty) S \mathbf{e}_j = \sum_{p=1}^M v_{ip}^t \sum_{r=1}^M u_{pr}^t s_{rj} \exp(\alpha_p^t y), \\ b_{k,l}(i, j, y; S, T) &\triangleq \mathbf{e}_i^T \int_0^y \exp(Tx) \mathbf{e}_k \mathbf{e}_l^T \exp(T(y-x)) S \mathbf{e}_j dx \\ &= \sum_{p=1}^M v_{ip}^t u_{pk}^t v_{lp}^t \sum_{r=1}^M u_{pr}^t s_{rj} y \exp(\alpha_p^t y) \\ &\quad + \sum_{p=1}^M \sum_{q \neq p}^M v_{ip}^t u_{pk}^t v_{lq}^t \sum_{r=1}^M u_{qr}^t s_{rj} \frac{\exp(\alpha_p^t y) - \exp(\alpha_q^t y)}{\alpha_p^t - \alpha_q^t}, \end{aligned}$$

where \mathbf{e}_i is the i th unit column vector and T represents the transpose.

Given rate matrices (S, T) and (i, j, y) , the conditional expectations of Z_k , $M_{k,l}$ and $N_{k,l}$ are given by

$$\begin{aligned} E_{(S,T)}[Z_k | i, j, y] &= \frac{b_{k,k}(i, j, y; S, T)}{a_j(i, y; S, T)}, & E_{(S,T)}[M_{k,l} | i, j, y] &= \frac{b_{k,l}(i, j, y; S, T)}{a_j(i, y; S, T)} t_{k,l}, \\ E_{(S,T)}[N_{k,j} | i, j, y] &= \frac{\mathbf{e}_i^T \exp(Ty) \mathbf{e}_k s_{k,j}}{a_j(i, y; S, T)}. \end{aligned}$$

• E-step

Under the condition of the estimated matrices $(S, T)^{[\tau]}$ of the τ th iteration and observed data $\{(i^\nu, j^\nu, y^\nu) \mid \nu = 1, \dots, N\}$, $Z_k^{[\tau+1]}$, $M_{kl}^{[\tau+1]}$ and $N_{kl}^{[\tau+1]}$ are estimated as follows:

$$Z_k^{[\tau+1]} = \sum_{\nu=1}^N E_{(S,T)^{[\tau]}}[Z_k^\nu | i^\nu, j^\nu, y^\nu], \quad M_{kl}^{[\tau+1]} = \sum_{\nu=1}^N E_{(S,T)^{[\tau]}}[M_{kl}^\nu | i^\nu, j^\nu, y^\nu],$$

$$N_{kl}^{[\tau+1]} = \sum_{\nu=1}^N E_{(S,T)^{[\tau]}}[N_{kl}^{\nu} | i^{\nu}, j^{\nu}, y^{\nu}].$$

• M-step

From $Z_k^{[\tau+1]}$, $M_{kl}^{[\tau+1]}$ and $N_{kl}^{[\tau+1]}$, the maximum likelihood estimators of the elements of $(S, T)^{[\tau+1]}$ are given by

$$s_{k,j}^{[\tau+1]} = \frac{N_{k,j}^{[\tau+1]}}{Z_k^{[\tau+1]}}, \quad t_{k,l}^{[\tau+1]} = \frac{M_{k,l}^{[\tau+1]}}{Z_k^{[\tau+1]}}, \quad t_{k,k}^{[\tau+1]} = - \sum_{l \neq k} t_{k,l}^{[\tau+1]} - \sum_{l=1}^M s_{k,l}^{[\tau+1]}.$$

D. A TSMAP

A TSMAP is defined as a MAP whose underlying process has a tree structure in [22]. For a real z , the eigenvalue $\alpha_i(z)$ is real and under Assumption 2, three spectral methods discussed in Propositions 1, 2 and in Appendix C are implemented as follows:

1. The matrix G : Zeros z_i ($i = 1, \dots, M$) are obtained by a bisection method and corresponding null vectors $\boldsymbol{\eta}_i$ are inductively calculated.
2. The stationary probability: Using the Fourier inversion transform, eigenvalues $\alpha_i(\omega^k)$ ($i = 1, \dots, M$) on the unit circle are inductively calculated by the Duran-Kerner-Aberth (DKA) method and corresponding eigenvectors are inductively calculated.
3. The EM algorithm: For the matrix T , eigenvalues α_i^t ($i = 1, \dots, M$) are obtained by a bisection method and corresponding left and right eigenvectors \boldsymbol{u}_i^t and \boldsymbol{v}_i^t are inductively calculated.

References

- [1] A. T. Andersen and B. F. Nielsen: A Markovian approach for modeling packet traffic with long range dependence. *IEEE Journal on Selected Areas in Communications*, **16** (1998), 719-732.
- [2] S. Asmussen: Phase-type distributions and related point processes: Fitting and recent advances. In S. Chakravarty and A. Alfa (eds.): *Matrix-Analytic Methods in Stochastic Models* (Marcel Dekker, New York, 1997), 137-149.
- [3] S. Asmussen, O. Nerman and M. Olsson: Fitting phase-type distributions via the EM algorithm. *Scandinavian Journal of Statistics*, **23** (1996), 419-441.
- [4] D. Bini and B. Meini: On cyclic reduction applied to a class of Toeplitz-like matrices arising in queueing problems. In W. J. Stewart (ed.): *Computations with Markov Chains* (Kluwer Academic Publisher, Boston, 1995), 21-38.
- [5] D. Bini and B. Meini: On the solution of a nonlinear matrix equation arising in queueing problems. *SIAM Journal on Matrix Analysis and Applications*, **17** (1996), 906-926.
- [6] G. L. Choudury, D. M. Lucantoni and W. Whitt: Squeezing the most out of ATM. *IEEE Transactions on Communications*, **44** (1996), 203-217.
- [7] P. J. Courtois: *Decomposability: Queueing and Computer System Applications* (Academic Press, London, 1977).
- [8] A. Elwalid and D. Mitra: Markovian arrival and service communication systems: Spectral expansions, separability and Kronecker-product forms. In W. J. Stewart (ed.): *Computations in the Markov Chains* (Kluwer Academic Publisher, Boston, 1995), 507-546.

- [9] H. R. Gail, S. L. Hantler and B. A. Taylor: Solutions of the basic matrix equation for $M/G/1$ and $G/M/1$ type Markov chains. *Communications in Statistics -Stochastic Models*, **10** (1994), 1-43.
- [10] H. R. Gail, S. L. Hantler and B. A. Taylor: Spectral analysis of $M/G/1$ and $G/M/1$ type Markov chains. *Advances in Applied Probability*, **28** (1996), 114-165.
- [11] H. R. Gail, S. L. Hantler and B. A. Taylor: Non-skip-free $M/G/1$ and $G/M/1$ type Markov chains. *Advances in Applied Probability*, **29** (1997), 733-758.
- [12] H. Heffes and D. M. Lucantoni: A Markov modulated characterization of packetized voice and data traffic and related statistical multiplexer performance. *IEEE Journal on Selected Areas in Communications*, **4** (1986), 856-868.
- [13] W. Leland, M. Taqqu, and W. Willinger: On the self-similar nature of Ethernet traffic (extended version). *IEEE/ACM Transactions on Networking*, **2** (1994), 1-15.
- [14] D. M. Lucantoni: New results on the single server queue with a batch Markovian arrival process. *Communications in Statistics: Stochastic Models*, **7** (1991), 1-46.
- [15] B. Meini: An improved FFT-based version of Ramaswami's formula. *Communications in Statistics: Stochastic Models*, **13** (1997), 223-238.
- [16] I. Mitrani: The spectral expansion solution method for Markov processes on lattice strips. In J. H. Dshalalow (ed.): *Advances in Queueing Theory, Methods, and Open Problems* (CRC Press Inc., Florida, 1995), 337-352.
- [17] S. Narayana and M. F. Neuts: The first two moment matrices of the counts for the Markovian arrival process. *Communications in Statistics: Stochastic Models*, **8** (1992), 459-477.
- [18] M. F. Neuts: A versatile Markovian point process. *Journal of Applied Probability*, **16** (1979), 764-769.
- [19] M. F. Neuts: *Structured Stochastic Matrices of $M/G/1$ Type and Their Applications* (Marcel Dekker Inc., New York, 1989).
- [20] S. Nishimura: Eigenvalue expression for mean queue length of $BMAP/G/1$ queue. *Asia-Pacific Journal of Operational Research*, **15** (1998), 193-202.
- [21] S. Nishimura: A spectral analysis for a $MAP/D/N$ queue. In G. M. Latouche and P. Taylor (eds.): *Advances in Algorithmic Methods for Stochastic Models* (Notable Publications Inc., New Jersey, 2000), 279-294.
- [22] S. Nishimura: Spectral methods for a tree structure MAP . In G. M. Latouche and P. Taylor (eds.): *Matrix-Analytic Methods* (World Scientific, New Jersey, 2002), 291-310.
- [23] S. Nishimura: A $MAP/G/1$ queue with an underlying birth-death process. *Stochastic Models*, **19** (2003), 425-447.
- [24] S. Nishimura and Y. Jiang: Spectral of matrix generating function for a $MAP/SM/1$ queue. *Communications in Statistics: Stochastic Models*, **16** (2000), 99-120.
- [25] S. Nishimura and H. Sato: Eigenvalue expression for a batch Markovian arrival process. *Journal of the Operations Research Society of Japan*, **40** (1997), 122-132.
- [26] V. Paxson and S. Floyd: Wide-area traffic: the failure of Poisson modeling. *IEEE/ACM Transactions on Networking*, **3** (1995), 226-244.
- [27] S. Robert and J. Y. Le Boudec: On a Markov modulated chain exhibiting self-similarities over finite timescale. *Performance Evaluation*, **27-28** (1996), 159-173.
- [28] H. Sato and S. Nishimura: Time-dependent moments of the counts on a $BMAP$. *Mathematical and Computer Modelling*, **31** (2000), 307-312.

- [29] H. A. Simon and A. Ando: Aggregation of variables in dynamic systems. *Econometrica*, **29** (1961), 111-138.

Shoichi Nishimura
Department of Mathematical Information Science
Tokyo University of Science
1-3, Kagurazaka, Shinjuku-ku
Tokyo, JAPAN, 162-8601
E-mail: nishimur@rs.kagu.tus.ac.jp